Available online at www.sciencedirect.com
SCIENCE DIRECT®
Bioorganic & Medicinal Chemistry 13 (2005) 2423–2430
Bioorganic & Medicinal Chemistry

Stabilization of guanine quadruplex DNA by the binding of porphyrins with cationic side arms

Takeshi Yamashita, Tadayuki Uno and Yoshinobu Ishikawa*

Graduate School of Pharmaceutical Sciences, Kumamoto University, 5-1 Oe-honmachi, Kumamoto 862-0973, Japan

Received 24 December 2004; revised 24 January 2005; accepted 24 January 2005

Abstract—Many aromatic ligands, including tetra-(*N*-methyl-4-pyridyl)porphyrin (TMPyP4), have been reported to bind and stabilize quadruplex structure of telomeric DNA. We synthesized novel quadruplex-interacting porphyrins with cationic pyridinium and trimethylammonium arms at *para*- or *meta*-position of all phenyl groups of tetratolyl porphyrin. An antiparallel quadruplex structure was found to be stabilized more greatly by the *meta*-isomers than by the *para*-isomers and well-studied TMPyP4, as revealed by the increase in melting temperature of the quadruplex. One mole equivalent of the isomers was sufficient to stabilize the quadruplex. From the results of absorption, induced circular dichroism, and fluorescence resonance energy transfer spectroscopic methods, the unique site for the porphyrin binding is suggested to be the external guanine tetrad or groove of the quadruplex. The cationic side arms played a key role in the stabilization of the quadruplex structure.

1. Introduction

Telomere is nucleoprotein structure at the end of chromosomes consisting of guanine-rich tandem repeats of the sequence d(TTAGGG) in human, the length of which ranges from 5000 to 15,000 basepairs with a single-stranded 3′ overhang of 100–200 bases.[1–3] Telomere has a key function in protecting chromosome ends from degradation, recombination, and end-to-end fusion.[3,4] Since RNA primer part is absent in replication at the end of chromosomes in normal somatic cells, telomere is shortened by 50–200 bases whenever cell division happens (end-replication problem),[5,6] and this erosion induces apoptosis when its length became critically short. On the other hand, telomerase is active in 85–90% of human tumor cells,[7,8] and this enzyme combines and elongates telomeres by catalyzing the addition of telomere sequence, maintaining telomere length so that these cells are immortalized.[8–12] Telomerase is composed of two major parts. One is a reverse transcriptase catalytic subunit, and the other is an RNA template that contains an 11 base sequence complementary to the telomeric guanine-rich sequence. Telomerase is closely related to tumorigenesis,[13] and hence telomerase is a target for the design of new anti-cancer drugs.[14] There are a number of approaches to telomerase inhibition; antisence oligonucleotides that target telomerase RNA template,[15,16] transfection of dominant-negative hTERT, which is the catalytic domain of human telomerase,[17,18] and blocking of interaction between telomerase and telomere by small molecules.[19–27]

Guanine-rich single-stranded overhang at the ends of chromosomes can be folded to form quadruplex structures under physiological conditions.[28,29] Quadruplex structures consist of two portions. One is a TTA loop and the other is a guanine-tetrad formed by cyclic Hoogsteen-type hydrogen bonding of four guanines (Fig. 1, A and B). A nuclear magnetic resonance (NMR) analysis revealed that the TTA loops of a quadruplex structure run diagonally and laterally at the end of guanine-tetrad, and four strands are arranged in an antiparallel fashion (Fig. 1A).[28] On the other hand, in a crystal structure all the TTA loops cross the side of guanine-tetrad diagonally and four strands are in a parallel arrangement.[29] Moreover, in the solution and in the crystal structure, three guanine-tetrads are stacked linearly by π–π interaction, and that metal ions are accommodated in the space between the guanine planes. Stabilization of the quadruplex structure inhibits its hybridization with a complementary single-stranded RNA template in telomerase, and hence telomerase

Keywords: Porphyrin; Quadruplex DNA; Melting temperature; CD; FRET.
* Corresponding author. Tel.: +81 96 371 4351; fax: +81 96 371 4350; e-mail: ishikawa@gpo.kumamoto-u.ac.jp

0968-0896/$ - see front matter © 2005 Elsevier Ltd. All rights reserved.
doi:10.1016/j.bmc.2005.01.041

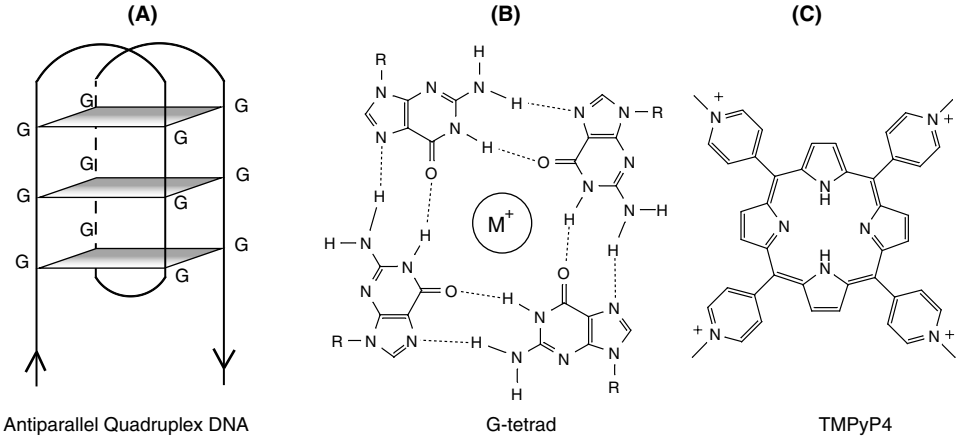

Figure 1. (A) Schematic representation of antiparallel quadruplex DNA. Arrows represent the direction (5′–3′) of the sugar phosphate backbone. (B) Chemical structure of G-tetrad formed by Hoogsteen-type hydrogen bonding network (- - -). A metal (K^+ or Na^+) is accommodated at the center of the G-tetrad. (C) Chemical structure of TMPyP4.

can no longer elongate telomere tandem repeats.[30] Some ligands including anthraquinones,[21–23] quinoacridines,[24] phenanthrolines,[25] substituted triazines,[26] and acridines[27] bind outside on the guanine-tetrad in a face-to-face manner by π–π stacking interaction. Thus, the size for the ligand chromophores is important in stabilizing quadruplex structures.[31–34]

One of the ligands that stabilize quadruplex DNA is 5,10,15,20-tetra-(*N*-methyl-4-pyridyl)porphyrin (TMPyP4) (Fig. 1C).[35–38] It is reported that TMPyP4 has a high affinity to quadruplex DNA and a high inhibition activity to telomerase. It binds externally to the end of quadruplex DNA with its porphyrin ring stacked on the guanine-tetrad, and the four peripheral pyridinium groups are located in the groove of quadruplex DNA. The size of the porphyrin ring of TMPyP4 is almost the same as the guanine-tetrad, and hence the stabilization of quadruplex DNA by TMPyP4 is due mainly to π–π stacking interaction between the porphyrin ring and the guanine-tetrad. On the other hand, 5,10,15,20-tetra-(*N*-methyl-2-pyridyl)porphyrin (TMPyP2), which is a positional isomer of TMPyP4, is less effective in telomerase inhibition activity than TMPyP4.[36,38] Thus, telomerase inhibition activity is greatly influenced by the position of the cationic substitution groups on the porphyrin periphery as well as by π–π stacking interaction.

Since stabilization of the quadruplex structure of the telomeric repeats is a viable way of inhibiting telomerase and leading cancer cells to apoptosis, we newly designed and synthesized four porphyrins with cationic side arms. As shown in Figure 2, *p*Tm and *p*Py have cationic trimethylammonium and pyridinium groups at the *para*-position of the tolyl groups, respectively. They have longer side arms than well-studied TMPyP4. On the other hand, *m*Tm and *m*Py are the positional isomers with cationic trimethylammonium and pyridinium side arms at the *meta*-position, respectively. On the basis of the measurement of thermal melting of an antiparallel quadruplex, the *meta*-isomers were found to greatly stabilize the quadruplex structure. The porphyrin binding modes

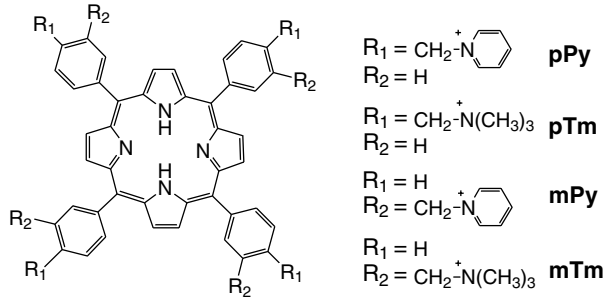

Figure 2. Chemical structures of *p*Py, *p*Tm, *m*Py, and *m*Tm.

were investigated spectroscopically by absorption, circular dichroism (CD), and fluorescence resonance energy transfer (FRET) methods, and we finally propose two alternative mechanisms for the porphyrin binding in the stabilization of the unique quadruplex structure.

2. Results

2.1. Thermal melting

Antiparallel quadruplex structures, including G4 DNA (see Section 5.1), show a characteristic positive CD peak at 295 nm and a negative CD peak at 260 nm.[39,40] Since the melted DNA structures fail to show the peak at 295 nm, the thermal stability of the quadruplex structures can be investigated by the temperature dependence of the positive CD peak.[41] Figure 3A typically shows normalized ellipticity changes of G4 DNA against temperature. Clearly, the profile shifted to higher temperature side in the presence of large amount of *m*Py. Melting temperature (T_m) was calculated from curve fitting. The T_m increases (ΔT_m) in G4 DNA/porphyrin complexes relative to that of free G4 DNA (51.7 °C) are plotted in Figure 3B against the mixing ratios of porphyrin to G4 DNA (r = [porphyrin]/[G4 DNA]). All the ΔT_m values increased sharply in the presence of porphyrins at $r < 1$, and reached almost maxima at $r = 1$ (TMPyP4, 4.8 °C; *p*Tm, 5.2 °C; *p*Py, 6.1 °C; *m*Tm,

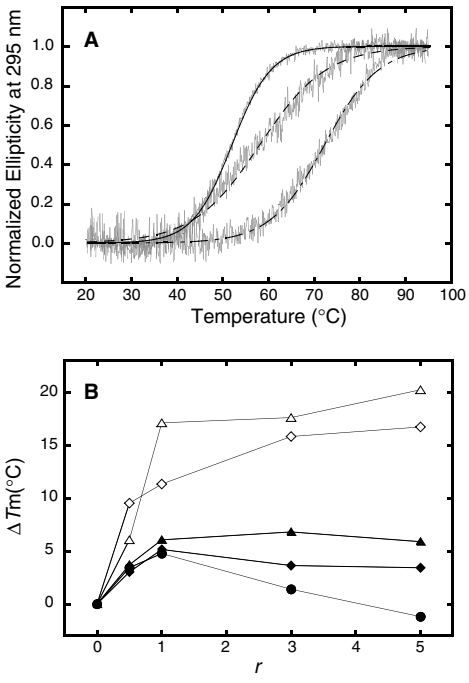

Figure 3. (A) Normalized elliptic changes of 5 μM G4 DNA at 295 nm against temperature in 4 mM Tris–HCl, 1 mM EDTA, and 100 mM KCl (pH 7.5). Fitting curves were drawn in the absence (——) or presence of 2.5 μM (r = 0.5, - - -) and 25 μM (r = 5, — - —) *m*Py. (B) The effect of r on the ΔT_m of G4 DNA in the presence of TMPyP4 (●), *p*Tm (◆), *p*Py (▲), *m*Tm (◇), and *m*Py (△).

11.4 °C; and *m*Py, 17.2 °C). Thus, the stabilization effect of the *meta*-isomers was greater than that of TMPyP4 and the *para*-isomers. The ΔT_m value for TMPyP4 decreased at $r > 1$, indicating that excess TMPyP4 destabilized the quadruplex structure. On the other hand, the ΔT_m values of the *para*-isomers at $r > 1$ remained essentially unchanged, and those of the *meta*-isomers increased slightly (Fig. 2B). It can be concluded that one molar equivalent of the porphyrins is sufficient for the stabilization of the quadruplex structure.

Among the synthetic porphyrins, two *meta*-isomers showed significantly higher ΔT_m values than the *para*-isomers. It indicates that the cationic side arms at the *meta*-position are significantly effective upon the stabilization of the quadruplex DNA. On the other hand, the ΔT_m values of *p*Py and *m*Py with pyridinium side arms were somewhat higher than those of *p*Tm and *m*Tm with trimethylammonium side arms, respectively (Fig. 3B). Therefore, the substitution group at the porphyrin periphery effected the stabilization of the quadruplex DNA to some extent. In order to gain insight into the stabilization mechanism, we measured absorption, induced CD, and FRET spectra of the porphyrins. It is reported that some ligands stabilizing quadruplex structure strongly have high telomerase inhibition activity.[42,43]

2.2. Absorption spectroscopy

Figure 4 shows the visible absorption spectra of TMPyP4 and *m*Py in the presence and absence of G4 DNA (r = 0.5). Under this condition, all the porphyrin

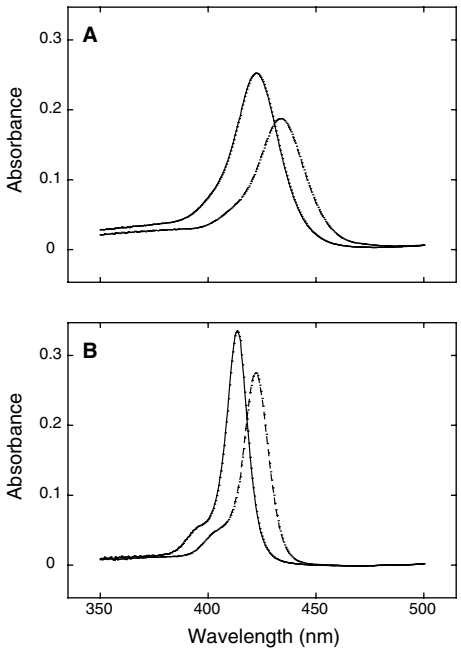

Figure 4. Absorption spectra of 1 μM TMPyP4 (A) and *m*Py (B) in the absence (——) or presence (- - -) of G4 DNA (r = 0.5). The spectra were recorded in 4 mM Tris–HCl, 1 mM EDTA, and 100 mM KCl (pH 7.5).

molecules are assumed to bind to a site responsible for the quadruplex stabilization (Fig. 3B). The Soret bands of all the porphyrins changed drastically upon addition of G4 DNA, and the observed bathochromic shifts ($\Delta\lambda$) and hypochromicities of the Soret bands (H) are summarized in Table 1. In the case of duplex DNA as a host, porphyrin intercalation is characterized experimentally by large bathochromic shift ($\Delta\lambda \geqslant 15$ nm) and substantial hypochromicity of the Soret band ($H \geqslant 35\%$). On the other hand, external groove binding mode of porphyrins is characterized by small bathochromic shift ($\Delta\lambda \leqslant 8$ nm) and hypochromicity ($H \leqslant 10\%$).[44] The observed $\Delta\lambda$ (9–12 nm) and H (18–35%) values of all the porphyrins were intermediate between those expected for intercalative and external groove binding modes, while both the $\Delta\lambda$ and H values were slightly larger for the *para*-isomers than those for the *meta*-isomers. Thus, these results suggest that the *para*- and *meta*-isomers bind to G4 DNA with a unique binding mode.

2.3. Induced CD spectroscopy

To clarify the binding mode, the induced CD spectra of the porphyrins were recorded at various concentrations

Table 1. Spectroscopic data for the porphyrins bound to G4 DNA

Porphyrin	$\Delta\lambda$ (nm)	H (%)
TMPyP4	12	26
*p*Tm	10	30
*p*Py	11	35
*m*Tm	9	25
*m*Py	9	18

$\Delta\lambda$, bathochromic shift. Hypochromicity (H) was determined by the equation $H = (\varepsilon_f - \varepsilon_b) \times 100/\varepsilon_f$, where ε_f and ε_b represent the molar absorptivities of free and bound porphyrins, respectively.

of G4 DNA. Although all of the cationic porphyrins are achiral, CD signals are induced once they bind to chiral DNA. Figure 5 shows the induced CD spectra of the cationic porphyrins bound to G4 DNA. In the case of duplex DNA, a positive induced CD band in the Soret region is indicative of groove binding, and a negative induced CD band indicates intercalation. Conservative CD signal is a signature of self-stacked porphyrins bound externally on the polymer surface.[44–47] Every porphyrin showed a positive peak in the Soret region in a low drug load ($r = 0.5$), suggesting that the porphyrins should locate at the groove of G4 DNA. The positive signals were observed even at $r = 1$, whereas the signal intensities were somewhat reduced. As the drug loads increased, however, the induced CD spectra of the porphyrins changed in complex manners. For example, the positive peak of TMPyP4 at $r = 0.5$ decreased gradually, resulting in a negative peak at $r = 5$. This signature suggests that TMPyP4 should intercalate between G-tetrads, supporting the binding mode previously proposed.[48] The CD spectra of *p*Tm, *p*Py, and *m*Py showed deformed positive and negative peaks at $r = 3$ and 5, suggesting multiple binding modes for these porphyrins. On the other hand, *m*Tm showed conservative CD profiles in the higher drug loads, suggesting external self-stacking binding mode on the G4 DNA surface. The binding mode of the porphyrins in the lower drug loads ($r \leqslant 1$) is commonly suggested to be external groove binding, whereas each porphyrin should bind to the quadruplex DNA in different manners in the higher drug loads.

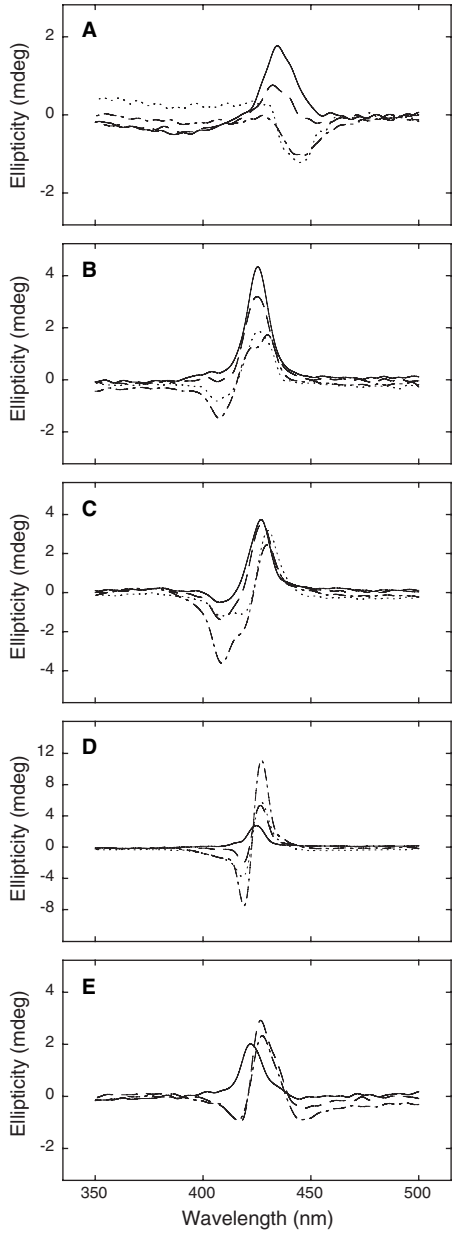

Figure 5. Induced CD spectra of 5 μM porphyrins in the presence of G4 DNA at $r = 0.5$ (——), 1 (- - -), 3 (· · ·), and 5 (- — - —). A, TMPyP4; B, *p*Tm; C, *p*Py; D, *m*Tm; and E, *m*Py. The spectra were recorded in 4 mM Tris–HCl, 1 mM EDTA, and 100 mM KCl (pH 7.5).

2.4. FRET spectroscopy

Fluorescence emission from porphyrins is weak when excited in a wavelength region between 240 nm and 320 nm, which is a DNA absorption region. Once porphyrins closely contact nucleobases, however, fluorescence is enhanced as a consequence of energy transfer from DNA bases to porphyrins. In general, FRET has been assumed to be observed specifically for a ligand intercalated between DNA basepairs.[49–54] Moreover, it was recently reported that FRET also occurs between DNA and porphyrins bound externally in the DNA groove.[55,56] Accordingly, the observation of FRET is indicative of the close contact of ligands with DNA bases. In addition, spectral profile of FRET should change depending on the type of a base, which closely interacts with ligands. Since G4 DNA consists of three types of bases (guanine, adenine, and thymine), we measured FRET from $(dG)_{12}$, poly(dA), and poly(dT) to the porphyrins. The FRET spectra of the single-stranded DNA/porphyrin complexes were compared with that of G4 DNA/porphyrin ones to know the base(s) in G4 DNA, where the bound porphyrin locates closely.

Figure 6A shows the FRET spectra of the single-stranded DNA/TMPyP4 complexes at selected concentrations of the single-stranded DNAs. Clearly, the spectra of poly(dT) and $(dG)_{12}$ showed stronger bands at relatively longer wavelength than that of poly(dA). The spectrum of $(dG)_{12}$ gave broad bands around 250 and 280 nm, which correspond to the absorption maxima of this polymer (a peak around 255 nm and a shoulder around 280 nm). The spectra of poly(dT) and poly(dA) gave bands around 275 nm and 260 nm, respectively, and these bands also correspond to the absorption maxima of the polymers at 267 nm and 258 nm, respectively. In the FRET spectra of the G4 DNA/porphyrin complexes, TMPyP4, *p*Py, and *m*Py showed maxima around 280 nm at $r = 0.5$, and *p*Tm and *m*Tm also showed maxima around 280 nm along with shoulders at shorter wavelength side. Thus, it is suggested that all the porphyrins should commonly locate close to guanine and/or thymine bases, because the FRET spectra of both guanine and thymine showed the bands around 280 nm (Fig. 6A).

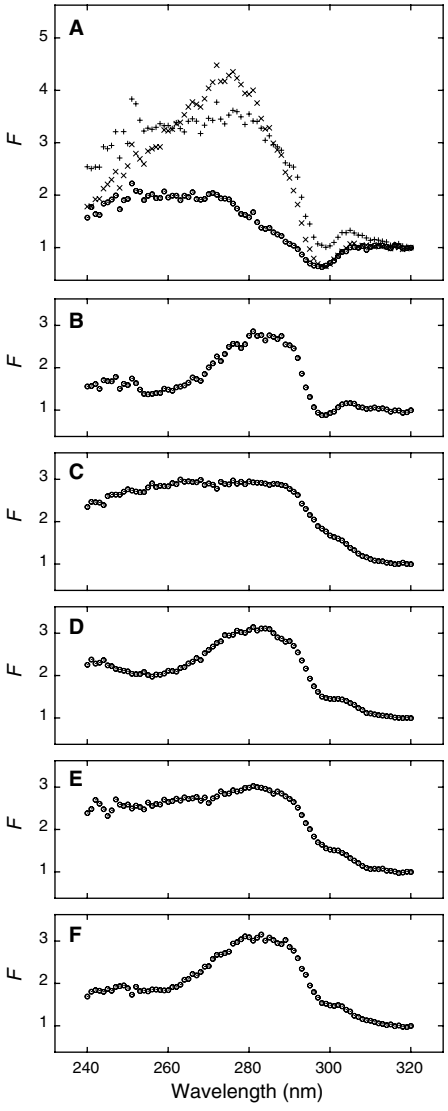

Figure 6. FRET spectra of TMPyP4 in the presence of poly(dA) (○), poly(dT) (×), and $(dG)_{12}$ (+) at a molar ratio of TMPyP4 to base of 1 to 10 (A), and of TMPyP4 (B), *p*Tm (C), *p*Py (D), *m*Tm (E), and *m*Py (F) in the presence of G4 DNA at $r = 0.5$ (○). *F* denotes relative fluorescence intensity. The spectra were recorded for 1 μM porphyrins in 4 mM Tris—HCl, 1 mM EDTA, and 100 mM KCl (pH 7.5).

3. Discussion

The T_m values of G4 DNA increased by the binding of the cationic porphyrins examined (Fig. 3B), indicating that the porphyrin ring contributes to the stabilization of the quadruplex structure. Especially noted is the fact that the *meta*-isomers with the cationic side arms were much more effective in the stabilization of the quadruplex structure than the *para*-isomers. In addition, the pyridinium side arms were preferable to the trimethylammonium ones in the stabilization, although the effect was moderate. Therefore, the position of the cationic side arms of the new porphyrins is mainly responsible for the significant stabilization of G4 DNA. The ΔT_m values for all the porphyrins were almost proportional to the drug loads between $r = 0$ and 1, and then reached plateau or decreased in the higher drug loads. This indicates that a crucial site for the porphyrin binding should exist for the stabilization of G4 DNA. Thus, we focus on the porphyrin binding manner at lower molar ratio in order to gain insight into the mechanism of the stabilization of the quadruplex structure.

Using induced CD and FRET spectroscopic methods, we characterized the mode of the porphyrins binding to G4 DNA. The spectral profiles of the induced CD and FRET studies for all the G4 DNA/porphyrin complexes at $r = 0.5$ were similar to each other, suggesting that the porphyrin rings should interact with G4 DNA at the same site. In the higher drug loads, however, the spectral profiles in induced CD differed markedly from those in the lower drug loads. Because the ΔT_m values of all the complexes were proportional to the r values at $0 \leqslant r \leqslant 1$, it is suggested that G4 DNA has a single unique site to be stabilized by the porphyrin binding. The excess porphyrins might bind to other binding site(s) of G4 DNA or interact with the porphyrin that bound G4 DNA. It should be noted that all the porphyrins shared the same binding site of G4 DNA at the lower molar ratio in spite of a large difference in both dimension and thickness of the porphyrins. The observed $\Delta\lambda$ and H values in the absorption spectra of the porphyrins were intermediate between those expected for intercalation and external groove binding. This observation suggests a binding mode different from intercalation between the G-tetrad planes, because π electrons of the porphyrins were moderately perturbed by the binding. It is most likely that the synthetic porphyrins are too bulky to be accommodated between the G-tetrad planes. On the other hand, the FRET spectra indicate that the bound porphyrins are located close to guanine and/or thymine bases. In addition, the induced CD spectra revealed a single positive peak at $r = 0.5$ for all the porphyrins, suggesting that the porphyrins locate in the groove of G4 DNA. Thus, the unique porphyrin binding mode is assumed to be one of two possibilities; external stacking to the end of the G-tetrad, or externally binding in the groove (Fig. 7).

It has been reported that many aromatic ligands, including TMPyP4, stack externally to the end of the G-tetrad as well as to the nearby diagonal loop, providing a unique binding site (Fig. 7A).[31–34,36] The moderate perturbation of π electrons of the porphyrins (Fig. 4) can be well explained by this model, since the porphyrins interact with only one face of the terminal G-tetrad, resulting in weaker π–π interaction in comparison with intercalation between G-tetrads. In this external stacking mode, the porphyrin ring should locate close to the guanine bases of G-tetrad, supporting the FRET results (Fig. 6). The cationic side arms of the porphyrins probably stabilize the quadruplex structure by reducing the electrostatic repulsion between the anionic phosphates of the backbone of the lateral or loops.[57] It is reported that an analogue of cryptolepine binds a parallel quadruplex DNA with this binding mode.[43] This external stacking model, however, fails to satisfy the result of the induced CD spectra (Fig. 5), although it is not clear at present what kind of spectrum is induced for this special binding mode. In addition, the synthetic porphyrins are so bulky

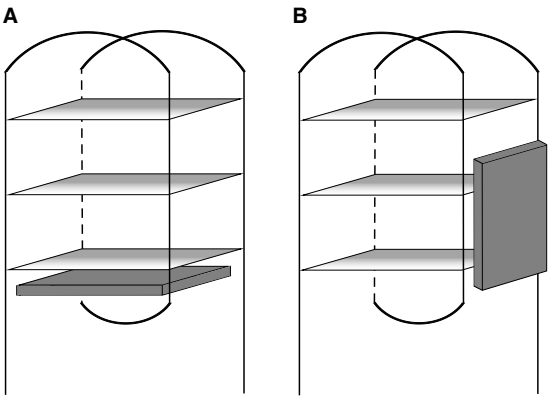

Figure 7. Schematic drawings of antiparallel quadruplex/porphyrin complex with external stacking (A) and groove binding mode (B). Porphyrins are illustrated as gray boxes.

that it is disadvantageous to approach to the external stacking site.

External groove binding mode is an alternative candidate (Fig. 7B), which is supported by the positive induced CD profile (Fig. 5). Antiparallel quadruplex DNA has one narrow, one wide, and two medium grooves.[58] Since two medium grooves are identical in their structure providing two equivalent binding sites, the single unique site for the porphyrin binding might locate in the narrow or wide groove. On the basis of the FRET results (Fig. 6), the porphyrin ring should locate close to the guanine and/or thymine, and hence the porphyrin presumably faces the quadruplex in the groove. In this face-on binding, the cationic side arms would interact electrostatically with the anionic phosphates of the guanine nucleotides. As a result of the relaxation of electrostatic repulsion between the anionic phosphate groups, the bonding of the G-tetrads should be strengthened, and hence resulting in the stabilization of the quadruplex structure as revealed by the increase in T_m. For the intermediacy of the $\Delta\lambda$ and H values, distortion of their porphyrin planes may account for the moderate perturbation of π electrons of the porphyrins.[59] Because the nucleobases are substantially buried, it should be difficult for the porphyrins to stack with the end of the G-tetrad (Fig. 4).

Our results strongly demonstrate that the interaction of the cationic side arms of the synthetic porphyrins with G4 DNA is very important whether the binding site is the external G-tetrad or the DNA groove. It is most likely that the cationic side arms of the *meta*-isomers direct upward from the porphyrin plane, and interact more effectively with the anionic phosphates than those of the *para*-isomers. This conformation is probably favorable for the stabilization of the quadruplex structure, allowing all four cationic groups to interact with the anionic phosphates in the loop and/or in the groove of the antiparallel quadruplex. Because the pyridinium side arms were preferred to the trimethylammonium ones in the stabilization, the aromatic and less bulky pyridinium groups might allow themselves both to interact with the anionic phosphates and to stack with bases in the DNA loop.

4. Conclusion

Many aromatic ligands have been reported to stabilize quadruplex DNA mainly by π–π stacking interaction with G-tetrad.[31–34] In this report, we have revealed that the newly synthetic cationic porphyrins stabilize antiparallel quadruplex DNA, and that the position of the cationic side arms of the tetratolyl porphyrins is very important in the stabilization of quadruplex structure. It is reported that telomerase inhibition activity of drugs is strongly related to the stabilization of quadruplex structure,[42,43] and hence *m*Tm and *m*Py are promising candidates for potent anti-cancer drugs. Further biochemical studies using telomerase and cancer cells will reveal the effectiveness of the novel porphyrins for cancer chemotherapy.

5. Experimental

5.1. Materials

Reagents for the synthesis of cationic porphyrins were purchased from Tokyo Chemical and Wako Pure Chemical Industries. Trimethylamine solution in ethanol (31–35%) was from Fluka. G4 DNA (5′-CATGGTGGTTTGGGTTAGGGTTAGGGTTAGGGTTACCAC-3′) and $(dG)_{12}$ oligomers were custom-synthesized, and poly(dA) and poly(dT) were from Sigma. The poly(dA) and poly(dT) concentrations were determined from the appropriate molar absorptivities: 9.1 $mM^{-1}cm^{-1}$ at 260 nm for poly(dA) in 1.0 mM sodium phosphate and 0.2 M NaCl (pH 7.0);[60] 8.52 $mM^{-1}cm^{-1}$ at 264 nm for poly(dT) in 10 mM sodium phosphate, 1 mM EDTA and 0.1 M NaCl (pH 7.0).[61] The tosylate salt of TMPyP4 was purchased from Dojin Chemical. 5,10,15,20-Tetrakis(α-bromo-*m*-tolyl)porphyrin (*m*BrTTP) and 5,10,15,20-tetrakis(α-bromo-*p*-tolyl)porphyrin (*p*BrTTP) were synthesized according to the procedure previously reported.[62,63]

5.2. 5,10,15,20-Tetrakis(α-pyridino-*p*-tolyl)porphyrin (*p*Py)

Forty milligrams of *p*BrTTP (0.045 mmol) was dissolved in 5 mL of pyridine and refluxed for 1.5 h with vigorous stirring. After cooling to room temperature, suspension was collected and dried. Yield: 51.0 mg (quantitative). ^{1}H NMR (DMSO-d_6): −2.99 (br s, 2, NH), 6.28 (s, 8, CH_2Br), 7.99 (d, 8, phenyl), 8.30 (d, 8, phenyl), 8.38 (t, 8, pyridine), 8.77–8.81 (m, 12, β-pyrrolic H, pyridine), 9.58 (d, 8, pyridine). $C_{68}H_{54}N_8Br_4{\cdot}7H_2O$ calcd: C, 57.16; H, 4.80; N, 7.84. Found: C, 57.10; H, 4.71; N, 7.67.

5.3. 5,10,15,20-Tetrakis(α-pyridino-*m*-tolyl)porphyrin (*p*Tm)

Fifty milligrams of *p*BrTTP (0.0507 mmol) was suspended in 10 mL of trimethylamine solution in ethanol (31–35%) and was heated to 80 °C for 14 h with vigorous stirring. After cooling to room temperature suspension was collected and dried. Yield: 35.3 mg (49.0%). ^{1}H NMR (DMSO-d_6): −2.94 (s, 2, NH), 3.37 (s, 36, CH_3),

4.96 (s, 8, CH_2Br), 8.01 (d, 8, H-3′,5′), 8.37 (d, 8, H-2′,6′), 8.94 (s, 8, β-pyrrolic H). $C_{60}H_{70}N_8Br_4{\cdot}11H_2O$ calcd: C, 50.71; H, 6.53; N, 7.89. Found: C, 50.86; H, 6.29; N, 7.82.

5.4. 5,10,15,20-Tetrakis(α-trimethylammonio-*p*-tolyl)-porphyrin (*m*Py)

Forty nine milligrams of *m*BrTTP (0.0497 mmol) was dissolved in 5 mL of pyridine and refluxed for 1.5 h with vigorous stirring. After cooling to room temperature, suspension was collected and dried. Yield: 59.0 mg (quantitative). ^{1}H NMR (DMSO-d_6): −3.00 (br s, 2, NH), 6.24 (m, 8, CH_2Br), 7.95 (m, 4, phenyl), 8.06 (br d, 4, phenyl), 8.25–8.32 (m, 12, phenyl, pyridine), 8.48 (m, 4, phenyl), 8.71 (m, 4, pyridine), 8.81 (br s, 8, β-pyrrolic H), 9.47 (m, 8, pyridine). $C_{68}H_{54}N_8Br_4{\cdot}5H_2O$ calcd: C, 58.64; H, 4.63; N, 8.04. Found: C, 58.70; H, 4.34; N, 8.11.

5.5. 5,10,15,20-Tetrakis(α-trimetylammonio-*m*-tolyl)-porphyrin (*m*Tm)

Fifty milligrams of *m*BrTTP (0.0507 mmol) was suspended in 10 mL of trimethylamine solution in ethanol (31–35%) and was heated to 80 °C for 14 h with vigorous stirring. After cooling to room temperature, suspension was collected and dried. Yield: 58.1 mg (80.6%). ^{1}H NMR (DMSO-d_6): −2.94 (s, 2, NH), 3.28 (s, 36, CH_3), 4.92 (s, 8, CH_2Br), 8.01 (t, 4, H-5′), 8.07 (d, 4, H-6′), 8.41 (br s, 8, H-2′,4′), 8.94 (s, 8, β-pyrrolic H). $C_{60}H_{70}N_8Br_4{\cdot}8H_2O$ calcd: C, 52.72; H, 6.34; N, 8.20. Found: C, 52.61; H, 6.10; N, 8.08.

5.6. Spectral measurements

Before the spectral measurements, G4 DNA was dissolved in 4 mM Tris–HCl, 1 mM EDTA, and 100 mM KCl (pH 7.5), and this solution was heated to 95 °C for 10 min and then cooled slowly to room temperature. DNA quadruplex is able to adopt two forms where the strand is folded in parallel and antiparallel, forming intramolecular G-quartets. Since the G4 DNA used in this study showed positive and negative CD peaks at 295 nm and 260 nm, respectively, G4 DNA was judged to shape antiparallel conformation as reported.[43,44] The CD peaks of G4 DNA were almost unaffected by the addition of the porphyrins, indicating that the antiparallel conformation was maintained throughout the spectroscopic measurements under our conditions. CD spectra were recorded on a Jasco J-720 spectropolarimeter. Melting curves of G4 DNA (5 μM) were obtained by tracing ellipticity at 295 nm, and temperature was raised from 20 to 95 °C at a rate of 0.5 °C/min with selected concentrations of the porphyrins. The value of *r* is defined as a molar ratio of porphyrin to G4 DNA. The induced CD spectra of the porphyrins (5 μM) were measured with selected concentrations of G4 DNA, and 20 independent spectra were averaged. The absorption spectra of the porphyrins (1 μM) were recorded on a Beckman DU640 spectrophotometer.

FRET spectra were recorded on a Hitachi F-4500 spectrophotometer. Excitation wavelength was scanned between 240 and 320 nm with selected concentrations of G4 DNA, poly(dA), poly(dT), and $(dG)_{12}$, and fluorescence emission from the porphyrins (1 μM) was observed at 660 nm. Relative fluorescence intensity (*F*) was calculated from the equation:

$$F = \left(\frac{I_\lambda}{I_{320}}\right)_b \left(\frac{I_{320}}{I_\lambda}\right)_f$$

where I_f and I_b are the fluorescence intensity of free and bound porphyrins, respectively. Fluorescence intensity excited at 320 nm was used for normalization because of the very low absorption of nucleic acids at this wavelength. Inner-filter effect was neglected since fluorescence intensity was proportional to porphyrin concentrations below 2 μM in our condition.

Acknowledgements

This work was supported by grants (Nos. 12771437 and 14771311 to Y.I.) for Science Research from the Japan Society for Promotion of Science.

References and notes

1. McElligott, R.; Wellinger, R. J. *EMBO J.* **1997**, *16*, 3705.
2. Wright, W. E.; Tesmer, V. M.; Huffman, K. E.; Levene, S. D.; Shay, J. W. *Gene Dev.* **1997**, *11*, 2801.
3. Blackburn, E. H. *Cell* **2001**, *106*, 661.
4. Ducray, C.; Pommier, J. P.; Martins, L.; Boussin, F. D.; Sabatier, L. *Oncogene* **1999**, *18*, 4211.
5. Levy, M. Z.; Allsopp, R. C.; Futcher, A. B.; Greider, C. W.; Harley, C. B. *J. Mol. Biol.* **1992**, *225*, 951.
6. Hastie, N. D.; Dempster, M.; Dunlop, M. G.; Thompson, A. M.; Green, D. K.; Allshire, R. C. *Nature* **1990**, *346*, 866.
7. Shay, J. W.; Bacchetti, S. *Eur. J. Cancer* **1997**, *33*, 787.
8. Urquidi, V.; Tarin, D.; Goodison, S. *Annu. Rev. Med.* **2000**, *51*, 65.
9. Greider, C. W.; Blackburn, E. H. *Cell* **1985**, *43*, 405.
10. Greider, C. W.; Blackburn, E. H. *Cell* **1987**, *51*, 887.
11. Greider, C. W.; Blackburn, E. H. *Nature* **1989**, *337*, 331.
12. Morin, G. B. *Cell* **1989**, *59*, 521.
13. Hanahan, D.; Weinberg, R. A. *Cell* **2000**, *100*, 57.
14. Counter, C. M.; Hirte, H. W.; Bacchetti, S.; Harley, C. B. *Proc. Natl. Acad. Sci. U.S.A.* **1994**, *91*, 2900.
15. Komata, T.; Kanzawa, T.; Kondo, Y.; Kondo, S. *Oncogene* **2002**, *21*, 656.
16. Norton, J. C.; Piatyszek, M. A.; Wright, W. E.; Shay, J. W.; Corey, D. R. *Nat. Biotechnol.* **1996**, *14*, 615.
17. Delhommeau, F.; Thierry, A.; Feneux, D.; Lauret, E.; Leclercq, E.; Courtier, M. H.; Sainteny, F.; Vainchenker, W.; Bennaceur-Griscelli, A. *Oncogene* **2002**, *21*, 8262.
18. Sachsinger, J.; Gonzalez-Suarez, E.; Samper, E.; Heicappell, R.; Muller, M.; Blasco, M. A. *Cancer Res.* **2001**, *61*, 5580.
19. Shin-ya, K.; Wierzba, K.; Matsuo, K.-i.; Ohtani, T.; Yamada, Y.; Furihata, K.; Hayakawa, Y.; Seto, H. *J. Am. Chem. Soc.* **2001**, *123*, 1262.
20. Kim, M. Y.; Vankayalapati, H.; Shin-ya, K.; Wierzba, K.; Hurley, L. H. *J. Am. Chem. Soc.* **2002**, *124*, 2098.
21. Sun, D.; Thompson, B.; Cathers, B. E.; Salazar, M.; Kerwin, S. M.; Trent, J. O.; Jenkins, T. C.; Neidle, S.; Hurley, L. H. *J. Med. Chem.* **1997**, *40*, 2113.

22. Perry, P. J.; Gowan, S.; Reszka, A. P.; Polucci, P.; Jenkins, T. C.; Kelland, L. R.; Neidle, S. *J. Med. Chem.* **1998**, *41*, 3253.
23. Perry, P. J.; Reszka, A. P.; Wood, A. A.; Read, M. A.; Gowan, S. M.; Dosanjh, H. S.; Trent, J. O.; Jenkins, T. C.; Kelland, L. R.; Neidle, S. *J. Med. Chem.* **1998**, *41*, 4873.
24. Heald, R. A.; Modi, C.; Cookson, J. C.; Hutchinson, I.; Laughton, C. A.; Gowan, S. M.; Kelland, L. R.; Stevens, M. F. G. *J. Med. Chem.* **2002**, *45*, 590.
25. Mergny, J.-L.; Lacroix, L.; Teulade-Fichou, M.-P.; Hounsou, C.; Guittal, L.; Hoarau, M.; Arimondo, P. B.; Vigneron, J.-P.; Lehn, J.-M.; Riou, J.-F.; Garestier, T.; Hélène, C. *Proc. Natl. Acad. Sci. U.S.A.* **2001**, *98*, 3062.
26. Riou, J.-F.; Guittat, L.; Mailliet, P.; Laoui, A.; Renou, E.; Petitgenet, O.; Mégnin-Chanet, F.; Hélène, C.; Mergny, J.-L. *Proc. Natl. Acad. Sci. U.S.A.* **2002**, *99*, 2672.
27. Read, M. A.; Harrison, R. J.; Romagnoli, B.; Tanious, F. A.; Gowan, S. H.; Reszka, A. P.; Wilson, W. D.; Kelland, L. R.; Neidle, S. *Proc. Natl. Acad. Sci. U.S.A.* **2001**, *98*, 4844.
28. Wang, Y.; Patel, D. J. *Structure* **1993**, *1*, 263.
29. Parkinson, G. N.; Lee, M. P.; Neidle, S. *Nature* **2002**, *417*, 876.
30. Zahler, A. M.; Williamson, J. R.; Cech, T. R.; Prescott, D. M. *Nature* **1991**, *350*, 718.
31. Fedoroff, O. Y.; Salazar, M.; Han, H.; Chemeris, V. V.; Kerwin, S. M.; Hurley, L. H. *Biochemistry* **1998**, *37*, 12367.
32. Gavathiotis, E.; Heald, R. A.; Stevens, F. G.; Searle, M. S. *Angew. Chem. Int. Ed.* **2001**, *40*, 4749.
33. Haider, S. M.; Parkinson, G. N.; Neidle, S. *J. Mol. Biol.* **2003**, *326*, 117.
34. Clark, G. R.; Pytel, P. D.; Squire, C. J.; Neidle, S. *J. Am. Chem. Soc.* **2003**, *125*, 4066.
35. Wheelhouse, R. T.; Sun, D.; Han, H.; Han, F. X.; Hurley, L. H. *J. Am. Chem. Soc.* **1998**, *120*, 3261.
36. Han, F. X.; Wheelhouse, R. T.; Hurley, L. H. *J. Am. Chem. Soc.* **1999**, *121*, 3561.
37. Han, H.; Langley, D. R.; Rangan, A.; Hurley, L. H. *J. Am. Chem. Soc.* **2001**, *123*, 8902.
38. Shi, D. F.; Wheelhouse, R. T.; Sun, D. Y.; Hurley, L. H. *J. Med. Chem.* **2001**, *44*, 4509.
39. Guo, Q.; Lu, M.; Kallenbach, N. R. *Biochemistry* **1993**, *32*, 3596.
40. Balagurumoorthy, P.; Brahmachari, S. K.; Mohanty, D.; Bansal, M.; Sasisekharan, V. *Nucleic Acids Res.* **1992**, *20*, 4061.
41. Miyoshi, M.; Nakano, A.; Sugimoto, N. *Biochemistry* **2002**, *41*, 15017.
42. Kerwin, S. M.; Sun, D.; Kern, J. T.; Rangan, A.; Thomas, P. W. *Bioorg. Med. Chem. Lett.* **2001**, *11*, 2411.
43. Guyen, B.; Schultes, C. M.; Hazel, P.; Mann, J.; Neidle, S. *Org. Biomol. Chem.* **2004**, *2*, 981.
44. Pasternack, R. F.; Gibbs, E. J.; Villafranca, J. J. *Biochemistry* **1983**, *22*, 5409.
45. Carvlin, M. J.; Mark, E.; Fiel, R.; Howard, J. C. *Nucleic Acids Res.* **1983**, *11*, 6141.
46. Carvlin, M. J.; Datta-Gupta, N.; Fiel, R. J. *Biochem. Biophys. Res. Commun.* **1982**, *108*, 66.
47. Carvlin, M. J.; Fiel, R. J. *Nucleic Acids Res.* **1983**, *11*, 6121.
48. Anantha, N. V.; Azam, M.; Sheardy, R. D. *Biochemistry* **1998**, *37*, 2709.
49. Scaria, P. V.; Shafer, R. H. *J. Biol. Chem.* **1991**, *266*, 5417.
50. Sehlstedt, U.; Kim, S. K.; Carter, P.; Goodisman, J.; Vollano, J. F.; Nordon, B.; Dabrowiak, J. C. *Biochemistry* **1994**, *33*, 417.
51. Sari, M. A.; Battioni, J. P.; Dupre, D.; Mansuy, D.; Le Pecq, J. B. *Biochemistry* **1990**, *29*, 4205.
52. Mergny, J. L.; Duval-Valentin, G.; Nguyen, C. H.; Perrouault, L.; Faucon, B.; Rougée, M.; Montenay-Garestier, T.; Bisagni, E.; Hélène, C. *Science* **1992**, *256*, 1681.
53. Haq, I.; Lincoln, P.; Suh, D.; Nordén, B.; Chowdhry, B. Z.; Chairs, J. B. *J. Am. Chem. Soc.* **1995**, *117*, 4788.
54. Le Pecq, J. B.; Paoletti, C. *J. Mol. Biol.* **1967**, *29*, 87.
55. Hyun, K. M.; Choi, S. D.; Lee, S.; Kim, S. K. *Biochim. Biophys. Acta* **1997**, *1334*, 312.
56. Yun, B. H.; Jeon, S. H.; Cho, T.-S.; Yi, S. Y.; Sehlstedt, U.; Kim, S. K. *Biophys. Chem.* **1998**, *70*, 1.
57. Risitano, A.; Fox, K. R. *Nucleic Acids Res.* **2004**, *32*, 2598.
58. Kerwin, S. M. *Curr. Pharm. Des.* **2000**, *6*, 441.
59. Parusel, A. B. J.; Wondimagegn, T.; Ghosh, A. *J. Am. Chem. Soc.* **2000**, *122*, 6371.
60. Pasternack, R. F.; Brigandi, R. A.; Abrams, M. J.; Williams, A. P.; Gibbs, E. J. *Inorg. Chem.* **1990**, *29*, 4483.
61. Uno, T.; Hamasaki, K.; Tanigawa, M.; Shimabayashi, S. *Inorg. Chem.* **1997**, *36*, 1676.
62. Bookser, B. C.; Bruice, T. C. *J. Am. Chem. Soc.* **1991**, *113*, 4208.
63. Jin, R.-H.; Aoki, S.; Shima, K. *Chem. Commun.* **1996**, 1939.